



# The Hidden Benefits of Limited Communication and Slow Sensing in Collective Monitoring of Dynamic Environments

Till Aust<sup>1,2</sup>(✉) , Mohamed S. Talamali<sup>3</sup> , Marco Dorigo<sup>1</sup> ,  
Heiko Hamann<sup>2</sup> , and Andreagiovanni Reina<sup>1</sup>(✉) 

<sup>1</sup> IRIDIA, Université Libre de Bruxelles, Brussels, Belgium  
mdorigo@ulb.ac.be, andreagiovanni.reina@ulb.be

<sup>2</sup> Institute of Computer Engineering, University of Lübeck, Lübeck, Germany  
till.aust@student.uni-luebeck.de, hamann@iti.uni-luebeck.de

<sup>3</sup> Sheffield Hallam University, Sheffield, UK  
s.talamali@shu.ac.uk

**Abstract.** Most of our experiences, as well as our intuition, are usually built on a linear understanding of systems and processes. Complex systems in general, and more specifically swarm robotics in this context, leverage non-linear effects to self-organize and to ensure that ‘more is different’. In previous work, the non-linear and therefore counter-intuitive effect of ‘less is more’ was shown for a site-selection swarm scenario. Although it seems intuitive that being able to communicate over longer distances should be beneficial, swarms were found to sometimes profit from communication limitations. Here, we build on this work and show the same effect for the collective perception scenario in a dynamic environment. We also find an additional effect that we call ‘slower is faster’: in certain situations, swarms benefit from sampling their environment less frequently. Our findings are supported by an intensive empirical approach and a mean-field model. All our experimental work is based on simulations using the ARGoS simulator extended with a simulator of the smart environment for the Kilobot robot called Kilogrid.

## 1 Introduction

In our recent research about information spreading in groups of individuals [30], we discovered a counter-intuitive mechanism by which reducing interactions between the individuals makes the group more capable to adopt new better opinions. This effect, that we call *less is more*, manifests when groups need to make consensus decisions and individuals follow a relatively simple voting behavior. Such conditions can be particularly relevant for the design of algorithms for swarms of minimalistic robots that make best-of- $n$  decisions [30]. Such algorithms are based on opinion dynamics models, in which every robot has an opinion about the option it currently considers the best (among  $n$  alternatives) and sends messages to neighboring robots to recruit them on that option [34].

In this study, we confirm the generality of our previous finding [30] by reproducing the *less is more* effect (LIME) in a different scenario: collective perception of an environmental feature, the so-called environmental element, in a dynamic environment. By studying this new scenario, we can control the speed of robot recruitment, that is the key parameter to trigger the LIME. Controlling this parameter was not possible in the previous study of Talamali et al. [30] as the recruitment speed was constrained by robot travel times to specific locations. These times also had high variance and depended, for example, on traffic congestion and robot density. The new scenario allows for a simplified analysis. Our results confirm and clarify the mechanisms. More importantly, we found a new surprising effect that was not reported earlier in this type of systems: the *slower is faster* effect [9, 18, 25–27] (SIFE). To adapt faster, recruited robots must be slower in disseminating their opinions and recruiting other robots. This is a second surprising and counter-intuitive mechanism of this simple voting system. The SIFE occurs when individuals are sparsely connected and make noisy estimates—two conditions commonly found in swarm robotics [10].

With this paper, we also release open-source code [2] supporting realistic simulations of the Kilogrid platform [1] (technology for Kilobots [21] to operate in smart environments) in ARGoS [15]. This simulation code, combined with the ARGoS Kilobot plugin [14], allows the use of identical code in simulation and reality (both for Kilobots and Kilogrid). Despite the limited adoption of the Kilogrid in other research labs than IRIDIA (ULB), we believe that supporting realistic physics-based simulations can help spreading the technology and encourage collaborations between laboratories with and without such equipment.

## 2 Collective Perception in a Dynamic Environment

In this paper, the task of the robot swarm is to make a consensus decision in favor of the predominant element of the environment [33]. We assume that the robots can individually estimate each element concentration (i.e., an element’s relative frequency in the environment) to form their opinion which they share with each other. While individual estimates are noisy, the swarm collectively filters noise and converges to an accurate collective decision [33]. Individual estimation errors can be caused, for example, by simple error-prone sensing devices (readings distant from the ground truth, e.g., [11, 13]), spatial correlations (clustered information in localised areas rather than uniformly in the environment, e.g., [3, 4, 29]), and limited sensing range. Our simulations allow us to control sources and levels of sampling errors as well as to disentangle the impact of sampling errors from other system dynamics of interest (e.g., recruitment time).

We conveniently model the collective perception problem in a similar way as done previously [33]. The to-be-estimated environmental element is the predominant color of the ground which is comprised of squared tiles ( $5\text{ cm}^2$ ). We consider tiles with  $n = 2$  colors: blue  and yellow  (see Fig. 1a)<sup>1</sup>. The difficulty of the

<sup>1</sup> The current geopolitical situation motivated our choice of tile color  .

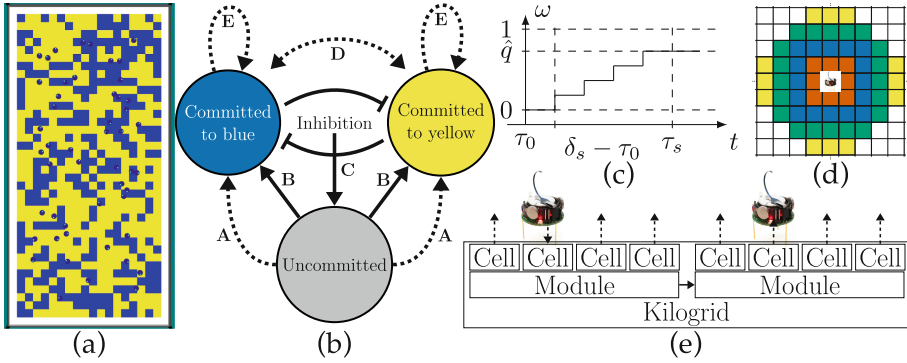


**Fig. 1.** (a) Collective perception scenario for the simulated Kilogrid in ARGoS (simulation code, see [2]), swarm of  $N = 50$  Kilobots (small black circles); (b) robots controlled by a finite state machine with  $n+1$  states (here  $n = 2$ ); transitions: self-sourced (dashed arrows) or social (solid arrows) evidence; uncommitted  $\rightarrow$  commit through (A) discovery or (B) recruitment; committed robots update their state by: (C) cross-inhibition, (D) direct switching, or (E) stay; (c) once recruited, robots gradually increase communication probability  $w$  for sampling time  $\tau_s = s \delta_s$ ,  $s$  samples every  $\delta_s$  seconds; (d) focal Kilogrid module receives Kilobot message and sends to all cells within communication range (proportional to parameter  $c$ ; communication range  $r_c$ ,  $c = \{2, 3, 4, 5\}$ ); (e) robot-to-robot communication is virtualised using Kilogrid. (Color figure online)

perception problem  $\kappa \in [0, 1]$  is determined by the ratio between the concentration of tiles in the two colors:  $\kappa = q_b/q_y$  where  $q_b$  and  $q_y$  are the concentrations of blue and yellow tiles, respectively. Without loss of generality we assume that yellow  $\blacksquare$  is the predominant color in all our experiments,  $q_y > q_b$ . The concentration of blue/yellow tiles corresponds to the number of blue/yellow tiles divided by the total number of tiles in the environment. The tiles are uniformly randomly distributed, hence reducing spatial correlations. However, spatial correlations exist within the area of a single tile. Indeed, taking several samples from the same tile results in biased measurements (see Sect. 5.2).

We consider a virtual dynamic scenario. In all our experiments, the most frequent color is yellow  $\blacksquare$ . However, the robot swarm is initialized to a state of full (100%) commitment in favor of blue  $\blacksquare$  with every robot holding an estimate  $q_b = 0.8$ . This increases the task difficulty and can be considered a sudden change of colors from blue to yellow ( $\blacksquare \rightarrow \blacksquare$ ) that happens right at the moment when we start our simulations. In the next section, we describe how robots reassess the environment’s state and reconsider their opinion.

### 3 A Minimalist Behavior for a Rich Collective Response

The robots have minimal requirements in terms of memory, computation, sensing, and communication capabilities. Compared with previous work that investigated decentralized consensus decision making in the collective perception sce-

nario, our algorithm has the fewest requirements, in line with our quest for minimalism. Different from previous work that required the storage of all available alternatives and all received messages [4, 23, 24], here the robots only store the information about a single opinion (i.e., the color considered predominant and its estimated concentration), the last received message from a neighbor, and a temporary variable to estimate possible environmental changes. Different from previous work requiring more advanced computation based on Bayesian inference [7, 8, 23, 24] or fusion operators from epistemic logic [4], our robot behavior is defined by a small finite state machine with reactive transitions. Different from previous work that required sensors capable of measuring a numerical value of the predominant element, such as an option quality, at every measurement step [7, 23, 24], here the robot can only sense the presence (■) or absence (not ■) of an element at a time. Different from previous work requiring maintenance of shared collective knowledge through rich inter-robot communication [28, 29], here the robots send simple messages with a few bits of information, only indicating their preferred element (i.e., their chosen color, for  $n = 2$  that is one bit of information). Other works in collective perception that are comparable to ours in their simplicity of individual robot requirements are Valentini et al. [33] and Zakir et al. [35]. We extend previous analyzes by considering a dynamic environment which has only been considered in a few consensus decision making studies for the site selection scenario [6, 16, 17, 30], while here we consider the collective perception scenario.

Despite the minimalist robot control algorithm and the robots' noisy measurements, the swarm is able to collectively gather and process the data to make accurate consensus decisions (picking the dominant color). The robot's control algorithm is based on simple reactive rules, relies on limited memory, and can be described as four routines that are executed in parallel: motion, opinion update, sampling, and broadcasting.

The **motion routine** is independent of the other parts of the robot's behavior. The robot's motion is neither influenced by its opinion nor by social or environmental inputs. The motion routine is a random walk implemented as a random waypoint mobility model [5, 30]. However, it could be substituted by any other algorithm implementing random diffusion. Using the random waypoint model, robots select random positions as their destinations. Once the destination is reached, robots select the next random destination. Robots avoid collisions with surrounding walls by selecting random destinations that are at least three robot-body lengths (approximately 10 cm) away from walls. As robot's motion is subject to noise, the robot can still approach walls. Once it gets at a distance smaller than three robot-body lengths from any wall, the robot starts a wall avoidance manoeuvre by rotating away from the wall and moving straight. The robots have no proximity sensing, therefore they do not implement any obstacle avoidance to prevent collisions with each other. To avoid robots remaining stuck in traffic jams caused by groups of robots moving in opposite directions (or robots not moving due to malfunctioning motors), robots select new random destinations if the previous destination was not reached within two minutes.

The **opinion update routine** is essential to solve the collective perception task because it determines how robots change their opinions and, hence, defines the collective behavior. Robots change their opinion so that a large majority of the swarm reaches an agreement on the predominant color. While we present this routine for  $n = 2$  colors, it does not require any changes to scale to numbers  $n > 2$ . Robots update their states every  $\tau_u = 2s$  following the cross-inhibition update shown in Fig. 1b. Robots can be in  $n + 1$  possible opinion states; in the investigated case of  $n = 2$  colors they can be committed to blue, committed to yellow, or uncommitted. Transitions between states are triggered by new self-sourced or social evidence. Self-sourced evidence (dashed arrows in Fig. 1b) is available when, after a period of length  $\tau_u$ , the robot completed sampling a color that is both different from and better than its current opinion (in case of uncommitted robots, any concentration estimate is considered as better). Hence, self-sourced evidence corresponds to discovering in the last  $\tau_u$  a color that seems more frequent than the color of its current opinion. Social evidence (solid arrows in Fig. 1b) is available when after a period of length  $\tau_u$  the robot received a message from a neighbor committed to a different color (if multiple messages have been received, only the most recent stays in memory). If both self-sourced and social evidence are available, the robot randomly selects one of the two, discarding the other. The new evidence triggers a state change: (a) committed robots with new social evidence become uncommitted—a *cross-inhibition* transition; (b) any robot with new self-sourced evidence becomes committed to the color corresponding to the new evidence—a *discovery* transition; (c) uncommitted robots with new social evidence, become committed as per the new evidence—a *recruitment* transition.

The **sampling routine** controls how information about the concentration of one element is collected from the environment. The robot continuously repeats sampling in cycles of collecting  $s$  samples. Each sample is a binary value indicating presence (1) or absence (0) of the environmental element of interest. Here, robots sample whether the color at their position is of a given color. The concentration estimate  $\hat{q}_i$  is the proportion between the number of samples  $s_i^+$  in which the element was present and the total number of samples  $s$ :  $\hat{q}_i = s_i^+/s$ . A new sampling cycle starts when the previous cycle has collected  $s$  samples, or when the robot changes opinion through social evidence. When the robot completes a sampling cycle or becomes uncommitted, it determines the new to-be-sampled color randomly. Here, the robot selects the color of the ground beneath itself. The random selection of the color to sample allows the robot either to update the color concentration estimate when it samples its commitment color, or to gather potential self-sourced evidence when it samples a different color. Instead, when a robot is recruited and commits to a new opinion  $i$ , it immediately starts to sample  $i$  to obtain the information needed to regulate its messaging frequency (weighted voting, as described in the broadcasting routine). This means that once a robot is recruited to  $i$ , it cannot instantaneously recruit other robots to  $i$  but a minimum amount of time is required to gather information about  $i$  first. The mathematical analysis of [30] showed that having this temporal delay between

change of opinion through recruitment and recruitment of other robots—the sampling time  $\tau_s$ —is the key mechanism that leads to the LIME. Therefore, the sampling time  $\tau_s$  is the control parameter of this study and it corresponds to  $\tau_s = s \delta_s$ , where  $\delta_s$  is the time between two samples. As analyzed in Sect. 5.2, the sampling parameters  $s$  and  $\delta_s$  are also linked to the estimation noise and have a determining impact on the collective dynamics.

The **broadcasting routine** implements a continuous ‘narrowcast’ of recruitment messages, that is, a broadcast to all robots within communication range  $r_c$  (i.e., neighbors). The robot scales its frequency of communication proportionally to the estimated concentration of the environmental element. The higher the estimated concentration of  $i$  is, the more recruitment messages for color  $i$  the robot sends. The robot sends a message with a frequency of  $w/\tau_m$  Hz where  $1/\tau_m = 2$  Hz is the maximum communication frequency of our robots and  $w = \min(2\hat{q}_i, 1)$  is the concentration weight for color  $i$ . We multiply by two ( $2\hat{q}_i$ ) because we need to find the predominant element and any concentration  $>50\%$  represents the absolute majority. For lower concentrations,  $w$  scales linearly between 0 and 1. While in case of  $n = 2$  a concentration  $<50\%$  indicates predominance of the other color, this does not generalize to  $n > 2$  and therefore we do not consider this deductive mechanism. A newly recruited robot does not have a concentration estimate yet. It gradually increments its communication frequency as it collects samples (see Fig. 1c). It computes  $w = \min(2\hat{q}_i, 1)$  using  $\hat{q}_i = s_i^+/s$  even if the collected samples are less than  $s$ . This mechanism helps avoiding situations of vocal minorities, that is, the situations in which a large proportion of the population changes their commitment and only a small proportion of robots communicates while the majority remain silent. In our implementation, just-recruited robots are not silent, yet less vocal. Uncommitted robots do not communicate until they get recruited or make a discovery transition.

## 4 Simulated Kilobots and Kilogrid

For our experiments, we use Kilobots which are cheap, simple, and small robots widely employed in swarm robotics [20–22, 31]. By regulating the frequency of two vibration motors, the Kilobots move on a flat surface at speeds of about 1 cm/s in roughly straight motion and rotate at the spot at about 45°/s. The Kilobot has a diameter of 3.3 cm, can display its internal state through a colored-LED, and can communicate with other robots and other devices through an infrared (IR) transceiver. The range of communication varies depending on lighting conditions and ground material [12]; in ideal conditions  $r_c \approx 10$  cm. The Kilobot’s control loop is executed at approximately 32 Hz.

Given these limited robot capabilities, researchers working with Kilobots have developed systems of augmented reality to allow Kilobots to interact with virtual environments [1, 19, 32]. We employ the Kilogrid system [32], which is a lattice of square electronic modules covered with a transparent glass. The Kilobots can move on the Kilogrid’s glass surface while communicating with static modules beneath which are equipped with the same IR transceivers as the

Kilobots. Each  $10 \times 10 \text{ cm}^2$  module is composed of four smaller  $5 \times 5 \text{ cm}^2$  square cells. In our setup, we use a  $1 \times 2 \text{ m}^2$  rectangular Kilogrid composed of  $10 \times 20$  modules for a total of 800 cells.

The collective perception scenario is implemented by assigning a color to each internal Kilogrid cell. In our environment there are 684 colored internal tiles and 116 non-colored tiles at the boundaries. Cells adjacent to walls are colorless because robots do wall avoidance when under two tiles away from any wall and should rarely visit these areas. All cells continuously signal their color to human observers using colored-LED and to the Kilobots via IR messages. The Kilogrid provides more information to the Kilobots to improve their movement which is subject to noise and unreliable [14]. The cell’s IR messages contain the color, the cell’s coordinates ( $x, y$  in the  $20 \times 40$  Kilogrid’s plane) and a wall flag. The coordinates are used to implement the above mentioned random waypoint mobility model [5, 30] to let robots effectively diffuse in space. The 0/1 wall flag indicates a wall at distance  $< 10 \text{ cm}$  and triggers wall avoidance.

The Kilogrid also allows extending the robot-to-robot communication range which is otherwise physically limited to  $r_c \approx 10 \text{ cm}$ . Our robots communicate with each other via the Kilogrid. They send their IR messages to the cell beneath them. The cell sends the message to all the cells at an Euclidean distance  $< c$  resulting in an effective range of  $r_c \approx 2.5 + 5(c - 1) \text{ cm}$  (see Figs. 1d, e). Hence, we can test communication ranges beyond the Kilobot’s limitations.

In this paper, we run experiments in simulation using an available ARGoS plugin that allows to run accurate simulations with the Kilobots [14], and a second ARGoS plugin for the simulation of the Kilogrid that we specifically developed for this study (open-source code available at [2]). The Kilogrid is programmed via code executed on each module. To simulate the Kilogrid, we developed an ARGoS loop function that runs the control cycle of all Kilogrid modules in each simulation step. Module-to-module communication is done by CAN bus, module-to-robot through IR messages, and modules can send data to the PC control station (e.g., log files). Following the ARGoS paradigm of using identical code for simulations and real-world experiments, we developed a simulated module interface that provides all functions available on the real Kilogrid module controller. The code for simulated and real modules has only minimal differences (documented in the code repository) that have been included to optimise simulation speed.

## 5 Results: Less is More and Slower is Faster

We test the ability of the robot swarm to adapt to sudden environmental changes. All robots start committed to blue ■ (predominant color before the change) with a high estimate  $q_b = 0.8$ , and hence  $w = 1$ . We assume the change ■  $\rightarrow$  ■ happens right at the beginning of our experiment, which is initialized with an environment with more yellow than blue tiles. The swarm is expected to perceive the change, reconsider its previous decision, and converge to a large majority (consensus decision) in favor of yellow. We consider the swarm capable to adapt to the

change when over a 5 min interval the mean of the number of robots committed to yellow is greater than 70% of the swarm size. In this way, we avoid to count short-lived random fluctuations as successful adaptations. Instead we want the swarm to reach a stable majority. The adaptation time is measured as the time it takes for at least 70% of the robots in the swarm to become committed to yellow at the beginning of the 5 min interval. We define “adaptation probability” as the proportion of simulation runs in which the swarm has successfully adapted. We run 30 simulations per condition.

### 5.1 When Recruitment is Slow do not be too Social, Less is More

We fix sample number  $s = 15$  and time between two samples  $\delta_s = 4s$ , and test different communication ranges  $2.5 \text{ cm} \leq r_c \leq 225 \text{ cm}$  for problem difficulties  $\kappa \in \{0.7, 0.8, 0.9\}$ . Hence, once recruited, robots broadcast with low probability the new color until they complete the sampling cycle which lasts  $\tau_s = s\delta_s = 60 \text{ s}$  (see broadcast frequency diagram in Fig. 1c). Because the positive feedback (i.e., recruited robots recruit other robots) is slow, we expect to observe similar dynamics as reported in [30]. Figure 2a shows that also here we have the LIME, where more social interactions (large  $r_c$ ) diminish the swarm’s ability to adapt. Therefore, we confirm the predictions of [30] and show this is a general effect that can take place in scenarios different from collective site selection, where it was first observed. This counter-intuitive effect can be explained via the social impact of committed subpopulations of unbalanced sizes. A large majority is able to repeatedly mute minorities that make temporary discoveries of alternative options. The minority’s opinion is slow to gain traction in the population as new recruits are slow in becoming vocal and are quickly reverted to the majority’s opinion. When the communication range is large, or equivalently when the robot density is high, any minority is in contact with the large majority at all time. Instead, sparse connectivity, due to a small communication range or a low robot density, reduces the importance of subpopulation sizes. Interactions are sporadic (often limited to pairs) and the collective dynamics are governed by opinion quality (encoded via messaging frequency).

Unlike the site selection scenario [30], where the positive feedback delay was hard to manipulate, here the delay consists in the sampling time  $\tau_s = s\delta_s$  and can easily be studied. We investigate how the collective performance varies for different sampling times and for different levels of robot connectivity. We study sampling time by varying values  $s$  as well as  $\delta_s$ , and robot connectivity by varying both communication range and robot density (proportional to swarm size as environment size is constant). Figs. 2b–d show that the LIME on robot connectivity is present in parameter regions of slow recruitment (top part of the plots) and gradually vanishes when recruitment is quick. This result is in agreement with theory, as quick recruitment enables positive feedback cascades and allows well connected swarms to react fast to environmental changes. While Figs. 2b–d only show results for problem difficulty  $\kappa = 0.9$ , we observed qualitatively equivalent dynamics for any  $\kappa$  tested.

We model the collective adaptation dynamics using a mean-field model built as a system of ODEs that describes the proportion of robots in each opinion state [30]. Let  $x_i$  be the proportion of robots committed to the environmental element  $i$  and let  $x_u$  be the proportion of uncommitted robots, with  $x_u + \sum_i x_i = 1$ . The opinion dynamics model reads as

$$\begin{aligned} \dot{x}_i = & \underbrace{\frac{q_i}{\tau_s} x_u}_A + \underbrace{\frac{1}{\tau_s} \frac{k r_c^2 N x_u}{1 + k r_c^2 N x_u} q_i x_i}_B - \underbrace{\frac{k r_c^2 N x_i}{1 + k r_c^2 N x_i} \sum_{j \neq i} q_j x_j}_C \\ & + \underbrace{\frac{q_i}{\tau_s} \sum_{j \neq i} [x_j \mathcal{H}(\hat{q}_i - \hat{q}_j)] - \frac{x_i}{\tau_s} \sum_{j \neq i} [q_j \mathcal{H}(\hat{q}_j - \hat{q}_i)]}_D, \end{aligned} \quad (1)$$

where  $\mathcal{H}$  is the unit step function, and  $k$  is a proportionality factor to fit the ODE system to the observed dynamics of the simulated swarm robotics system (e.g., speed of robots, communication frequency, robots' opinion update time). The four terms on the rhs of Eq. (1) model discovery, recruitment, cross-inhibition, and direct switching transitions (capital letters below each term correspond to the transitions depicted in Fig. 1b, for more details see [30]).

The model of Eq. (1), as previously published [30], describes 'slow' (i.e., not instantaneous) recruitment through the Holling function type 2. As the sampling time  $\tau_s$  is decreased, the recruitment becomes quicker and the effect of the Holling function reduces. As a result the recruitment rate becomes approximately linear on neighborhood size. Through bifurcation analysis in the case of  $n = 2$ , we identify two states of the system as a function of the communication range (in Fig. 2e), or equivalently of the swarm density (not shown). Prior to the subcritical bifurcation (low  $r_c$  or  $N$ ), the system has a single stable equilibrium that represents a consensus decision for the color with the highest concentration, therefore, in this parameter range adaptation is guaranteed. After the bifurcation (high  $r_c$  or  $N$ ), a second stable equilibrium appears representing a consensus decision for the inferior alternative. In this parameter range, the swarm when initialized at equilibrium for the inferior color can only switch between the coexisting attractors through high random fluctuations and the swarm may take longer to adapt. The bifurcation analysis of Fig. 2e shows results that are qualitatively equivalent to the dynamics observed in simulations (see Fig. 2g).

## 5.2 With Noisy Estimates and Few Neighbors, Slower is Faster

The results of Figs. 2b–d also show new interesting dynamics that were not found in the previous study [30]. When robot connectivity is low (i.e., sporadic social interactions) the swarm is only able to adapt when the sampling time is high (either the number of samples  $s$  or the time between readings  $\delta_s$  are large). This mechanism corresponds to the SIFE [9, 18, 25–27] by which the swarm is able to adapt at a quicker speed (i.e., within 40 min) when the robots perform their task of estimating the environmental element concentration at a slower pace.

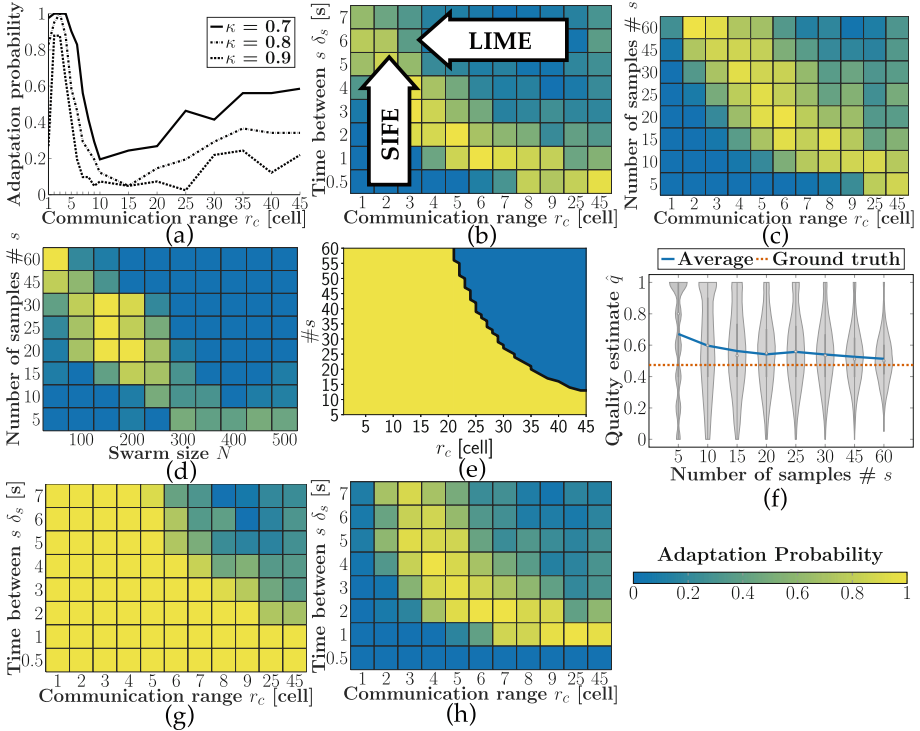


**Fig. 2.** (a, b, c) Smaller communication ranges lead to higher adaptation probability. This effect happens only when recruitment is slow, i.e., in the top part of panels (b, c), for high sampling times  $\tau_s = s \delta_s$ , which can be caused by (b) large times between samples  $\delta_s$  (with fixed  $s = 15$ ) or (c) high numbers of samples  $s$  (with fixed  $\delta_s = 1$ ). (b–c) When communication is limited, slower sampling time leads to higher probability of adapting. (d) The same two effects can be observed for fixed communication range ( $r_c \approx 12.5$  cm for  $c = 3$ ) and increasing robot density, which we control by modifying the swarm size  $N$  in an environment with a fixed size; (e) the ODE model (Eq. (1)) predicts results qualitatively similar to simulations without noise (g) ( $N = 50$ ,  $\kappa = 0.9$ ,  $k = 4 \times 10^{-6}$ ); (f) sampling times  $\tau_s$  influence the noise, because accuracy increases when robots collect more samples  $s$ ; (g) when estimation noise is independent of sampling and low ( $\sigma = 0$ ) the SIFE disappears; (h) when estimation noise is independent of sampling and high ( $\sigma = 0.1$ ) both effects are present; if not specified, swarm size  $N = 50$ , difficulty  $\kappa = 0.9$ , 30 simulations each; color-maps show probability to adapt.

To study this phenomenon, we ran additional simulations. Slowing down the sampling process has the double effect of slowing down the recruitment and of reducing errors on the color concentration. Increasing either the sample number  $s$  or the time between samples  $\delta_s$  reduces the estimation noise because the robot respectively collects more samples (see Fig. 2f) or reduces sample correlation. Therefore, we investigate whether adaptation of sparse swarms is limited by high noise or quick recruitment.

In additional simulations, robots estimate color concentration ( $\hat{q}_b$  or  $\hat{q}_y$ ) using a normal distribution rather than observing tile colors. The mean of the normal distribution is the correct concentration of the color in the environment and we test various standard deviations  $\sigma$  which represent the sampling noise. By disentangling noise from sampling time, we can study their impact separately. Without noise ( $\sigma = 0$ ), swarms with low communication range are able to adapt to changes, hence sampling time has no impact on the collective ability to adapt (see Fig. 2g). Interestingly, when noise is high ( $\sigma \in \{0.1, 0.2\}$ , Fig. 2h), swarms are only able to adapt when robots take a long time to make their estimate (i.e., recruited robots are slow in becoming recruiters themselves). The slower a robot starts disseminating its opinion, the faster its opinion spreads throughout the swarm. A supposed optimal sampling time (sampling rate) might also depend on environmental features (e.g., tile sizes).

Unfortunately, we cannot provide an explanation of this effect by theoretical analysis as done for the LIME. The mean-field model of Eq. (1) describes a noiseless system and cannot model the SIFE that is driven by noise. In future work we intend to study this phenomenon using stochastic models.

## 6 Conclusions

We have shown that our previous results [30] generalize to a different scenario: collective perception of dynamic environmental features. This scenario allows for a more in-depth analysis not possible in the previous scenario. We have clarified the relationship between recruitment speed and ability to collectively adapt to environmental changes. The collective task that we study here is equivalent to enabling the swarm to revise an incorrect collective decision that led the swarm to reach a consensus for the inferior alternative and avoids lock-in states.

Our results explain the importance of considering the interplay between sampling time and the communication range when designing the robot behavior as it can have a paramount effect on the collective dynamics. Through rigorous mathematical and computational analysis, we explain the mechanisms that cause the LIME, which is triggered by slow recruitment. During our investigations, we also stumbled upon a new effect: slower individual dissemination enables faster global agreement. We are unable, for the moment, to explain mathematically the SIFE. However, our computational analysis confirms that the results on speed are not confounded with estimation noise. Our future research will investigate the mechanisms causing such unexpected dynamics which are highly relevant for swarm robotics studies as they manifest when swarm connectivity is sparse and robots follow a simple behavior subject to high levels of noise.

**Acknowledgements.** The authors thank Anthony Antoun, Marco Trabattoni, and Jonas Kuckling for technical support concerning Kilogrid and simulations on HPC. MD and AR acknowledge support from the Belgian F.R.S.-FNRS, of which they are Research Director and Chargé de Recherches, respectively.

## References

1. Antoun, A., Valentini, G., Hocquard, E., Wiandt, B., Trianni, V., Dorigo, M.: Kilogrid: a modular virtualization environment for the Kilobot robot. In: 2016 IEEE/RSJ International Conference on Intelligent Robots and Systems (IROS), vol. 1, pp. 3809–3814. IEEE (2016). <https://doi.org/10.1109/IROS.2016.7759560>
2. Aust, T., Reina, A.: Open-source code for simulating the Kilogrid in ARGoS. [https://github.com/tilly111/adaptive\\_symmetry\\_breaking](https://github.com/tilly111/adaptive_symmetry_breaking)
3. Bartashevich, P., Mostaghim, S.: Benchmarking collective perception: new task difficulty metrics for collective decision-making. In: Moura Oliveira, P., Novais, P., Reis, L.P. (eds.) EPIA 2019. LNCS (LNAI), vol. 11804, pp. 699–711. Springer, Cham (2019). [https://doi.org/10.1007/978-3-030-30241-2\\_58](https://doi.org/10.1007/978-3-030-30241-2_58)
4. Bartashevich, P., Mostaghim, S.: Multi-featured collective perception with evidence theory: tackling spatial correlations. *Swarm Intell.* **15**(1), 83–110 (2021). <https://doi.org/10.1007/s11721-021-00192-8>
5. Bettstetter, C., Hartenstein, H., Pérez-Costa, X.: Stochastic properties of the random waypoint mobility model. *Wirel. Netw.* **10**(5), 555–567 (2004). <https://doi.org/10.1023/B:WINE.0000036458.88990.e5>
6. Soorati, M.D., Krome, M., Mora-Mendoza, M., Ghofrani, J., Hamann, H.: Plasticity in collective decision-making for robots: creating global reference frames, detecting dynamic environments, and preventing lock-ins. In: 2019 IEEE/RSJ International Conference on Intelligent Robots and Systems (IROS), vol. 1, pp. 4100–4105. IEEE (2019). <https://doi.org/10.1109/IROS40897.2019.8967777>
7. Ebert, J.T., Gauci, M., Mallmann-Trenn, F., Nagpal, R.: Bayes bots: collective Bayesian decision-making in decentralized robot swarms. In: 2020 IEEE International Conference on Robotics and Automation (ICRA), pp. 7186–7192. IEEE (2020). <https://doi.org/10.1109/ICRA40945.2020.9196584>
8. Ebert, J.T., Gauci, M., Nagpal, R.: Multi-feature collective decision making in robot swarms. In: Proceedings of the 17th International Conference on Autonomous Agents and Multiagent Systems (AAMAS), Richland, SC, vol. 3, pp. 1711–1719 (2018)
9. Gershenson, C., Helbing, D.: When slower is faster. *Complexity* **21**(2), 9–15 (2015). <https://doi.org/10.1002/cplx.21736>
10. Hamann, H.: *Swarm Robotics: A Formal Approach*. Springer, Cham (2018). <https://doi.org/10.1007/978-3-319-74528-2>
11. Lee, C., Lawry, J., Winfield, A.F.: Negative updating applied to the best-of-n problem with noisy qualities. *Swarm Intell.* **15**(1), 111–143 (2021). <https://doi.org/10.1007/s11721-021-00188-4>
12. Nikolaidis, E., Sabo, C., Marshal, J.A.R., Reina, A.: Characterisation and upgrade of the communication between overhead controllers and Kilobots. Technical report, White Rose Research Online (2017)
13. Parker, C.A.C., Zhang, H.: Biologically inspired decision making for collective robotic systems. In: 2004 IEEE/RSJ International Conference on Intelligent Robots and Systems (IROS) (IEEE Cat. No. 04CH37566), vol. 1, pp. 375–380. IEEE (2004). <https://doi.org/10.1109/IROS.2004.1389381>
14. Pinciroli, C., Talamali, M.S., Reina, A., Marshall, J.A.R., Trianni, V.: Simulating Kilobots within ARGoS: models and experimental validation. In: Dorigo, M., Birattari, M., Blum, C., Christensen, A.L., Reina, A., Trianni, V. (eds.) ANTS 2018. LNCS, vol. 11172, pp. 176–187. Springer, Cham (2018). [https://doi.org/10.1007/978-3-030-00533-7\\_14](https://doi.org/10.1007/978-3-030-00533-7_14)

15. Pinciroli, C., et al.: ARGoS: a modular, parallel, multi-engine simulator for multi-robot systems. *Swarm Intell.* **6**(4), 271–295 (2012). <https://doi.org/10.1007/s11721-012-0072-5>
16. Prasetyo, J., De Masi, G., Ferrante, E.: Collective decision making in dynamic environments. *Swarm Intell.* **13**(3), 217–243 (2019). <https://doi.org/10.1007/s11721-019-00169-8>
17. Prasetyo, J., De Masi, G., Ranjan, P., Ferrante, E.: The best-of- $n$  problem with dynamic site qualities: achieving adaptability with stubborn individuals. In: Dorigo, M., Birattari, M., Blum, C., Christensen, A.L., Reina, A., Trianni, V. (eds.) ANTS 2018. LNCS, vol. 11172, pp. 239–251. Springer, Cham (2018). [https://doi.org/10.1007/978-3-030-00533-7\\_19](https://doi.org/10.1007/978-3-030-00533-7_19)
18. Rahmani, P., Peruani, F., Romanczuk, P.: Flocking in complex environments-attention trade-offs in collective information processing. *PLoS Comput. Biol.* **16**(4), 1–18 (2020). <https://doi.org/10.1371/journal.pcbi.1007697>
19. Reina, A., Cope, A.J., Nikolaidis, E., Marshall, J.A.R., Sabo, C.: ARK: augmented reality for Kilobots. *IEEE Robot. Autom. Lett.* **2**(3), 1755–1761 (2017). <https://doi.org/10.1109/LRA.2017.2700059>
20. Reina, A., Ioannou, V., Chen, J., Lu, L., Kent, C., Marshall, J.A.: Robots as actors in a film: no war, a robot story. arXiv preprint [arXiv:1910.12294](https://arxiv.org/abs/1910.12294) (2019)
21. Rubenstein, M., Ahler, C., Hoff, N., Cabrera, A., Nagpal, R.: Kilobot: a low cost robot with scalable operations designed for collective behaviors. *Robot. Auton. Syst.* **62**(7), 966–975 (2014). <https://doi.org/10.1016/j.robot.2013.08.006>
22. Rubenstein, M., Cornejo, A., Nagpal, R.: Programmable self-assembly in a thousand-robot swarm. *Science* **345**(6198), 795–799 (2014). <https://doi.org/10.1126/science.1254295>
23. Shan, Q., Mostaghim, S.: Collective decision making in swarm robotics with distributed Bayesian hypothesis testing. In: Dorigo, M., et al. (eds.) ANTS 2020. LNCS, vol. 12421, pp. 55–67. Springer, Cham (2020). [https://doi.org/10.1007/978-3-030-60376-2\\_5](https://doi.org/10.1007/978-3-030-60376-2_5)
24. Shan, Q., Mostaghim, S.: Discrete collective estimation in swarm robotics with distributed Bayesian belief sharing. *Swarm Intell.* **15**(4), 377–402 (2021). <https://doi.org/10.1007/s11721-021-00201-w>
25. Slobodkin, L.B.: *Growth and Regulation of Animal Populations*. Holt, Rinehart and Winston, New York (1961)
26. Stark, H.U., Tessone, C.J., Schweitzer, F.: Decelerating microdynamics can accelerate macrodynamics in the voter model. *Phys. Rev. Lett.* **101**(1), 018701 (2008). <https://doi.org/10.1103/PhysRevLett.101.018701>
27. Stark, H.U., Tessone, C.J., Schweitzer, F.: Slower is faster: fostering consensus formation by heterogeneous inertia. *Adv. Complex Syst.* **11**(4), 551–563 (2008). <https://doi.org/10.1142/S0219525908001805>
28. Strobel, V., Castelló Ferrer, E., Dorigo, M.: Managing byzantine robots via blockchain technology in a swarm robotics collective decision making scenario. In: *Proceedings of the 17th International Conference on Autonomous Agents and Multiagent Systems (AAMAS)*, Richland, SC, vol. 3, pp. 541–549 (2018)
29. Strobel, V., Castelló Ferrer, E., Dorigo, M.: Blockchain technology secures robot swarms: a comparison of consensus protocols and their resilience to Byzantine robots. *Front. Robot. AI* **7**, 54 (2020). <https://doi.org/10.3389/frobt.2020.00054>
30. Talamali, M.S., Saha, A., Marshall, J.A.R., Reina, A.: When less is more: robot swarms adapt better to changes with constrained communication. *Sci. Robot.* **5**(56), eabf1416 (2021). <https://doi.org/10.1126/scirobotics.abf1416>

31. Valentini, G., Hamann, H., Dorigo, M.: Self-organized collective decision-making in a 100-robot swarm. In: Proceedings of the Twenty-Ninth AAAI Conference on Artificial Intelligence (AAAI 2015), pp. 4216–4217. AAAI Press (2015)
32. Valentini, G., et al.: Kilogrid: a novel experimental environment for the Kilobot robot. *Swarm Intell.* **12**(3), 245–266 (2018). <https://doi.org/10.1007/s11721-018-0155-z>
33. Valentini, G., Brambilla, D., Hamann, H., Dorigo, M.: Collective perception of environmental features in a robot swarm. In: ANTS 2016. LNCS, vol. 9882, pp. 65–76. Springer, Cham (2016). [https://doi.org/10.1007/978-3-319-44427-7\\_6](https://doi.org/10.1007/978-3-319-44427-7_6)
34. Valentini, G., Ferrante, E., Dorigo, M.: The best-of-n problem in robot swarms: formalization, state of the art, and novel perspectives. *Front. Robot. AI* **4**, 9 (2017). <https://doi.org/10.3389/frobt.2017.00009>
35. Zakir, R., Dorigo, M., Reina, A.: Robot swarms break decision deadlocks in collective perception through cross-inhibition. In: Dorigo, M., et al. (eds.) ANTS 2022. LNCS, vol. 13491, pp. 209–221. Springer, Cham (2022)